

Prediction of nanoparticles' size-dependent melting temperature using mean coordination number concept

Mostafa Mirjalili, Jalil Vahdati-Khaki *

Department of Materials and Metallurgical Engineering, Ferdowsi University of Mashhad, Mashhad 91775-1111, Iran

ARTICLE INFO

Article history:

Received 28 July 2007

Received in revised form

3 February 2008

Accepted 11 March 2008

Keywords:

A. Nanostructures

D. Surface properties

ABSTRACT

Many models have been developed to predict size-dependent melting temperature of nanoparticles. A new model based on the cluster mean coordination number (MCN) calculations is developed in this work. Results of the model for Al, Au, Pb, Ag, Cu, In, Sn, and Bi were compared with other models and experiments. The comparison indicated that the MCN model is in good agreement with available experimental values. It is also found that the melting temperature is more dependent on particle size as the atomic radius increased.

© 2008 Elsevier Ltd. All rights reserved.

1. Introduction

Nanomaterials are experiencing rapid development in recent years due to their known and/or potential applications in areas such as electronics, catalysis, ceramics, magnetic data storage, structural components, etc. Nanomaterials can be classified into nanocrystalline materials and nanoparticles. The former are polycrystalline bulk materials with grain sizes in the nanometer range, while the latter refers to ultrafine dispersive particles with diameters below 100 nm [1]. Parallel to developments in synthesis, processing, and application of nanomaterials, many researches are accomplished to explain and predict their behavior. In recent decades, researchers have paid more attention to the melting of nanosolids, because the melting temperatures of nanosolids are different from that of the corresponding bulk materials. Generally, models that predict nanoparticle melting temperature can be categorized into three groups according to their theory:

- models developed in terms of classical thermodynamics and surface energy [2–8],
- models based on molecular thermodynamics and atomic mean square displacement (msd) [9–11], and
- models established on cohesive energy calculations of particles [12–17].

Liquid-drop model developed by Nanda et al. [13] is a model based on cohesive energy calculations. In this model, the relation between melting point and particle size is

$$T_{mp} = T_{mb} \left(1 - \frac{\beta}{zD} \right) \quad (1)$$

where T_{mp} and T_{mb} are the melting temperature of the nanoparticle and the corresponding bulk material. β can be estimated for different elements using the known values of atomic volume, v_0 , surface energy, σ , and T_{mb} , via Eq. (2). It may be noted that z is the dimensional factor and has values 1, 3/2, and 3 for nanoparticles, nanowires, and thin films, respectively. D represents the diameter in case of nanoparticles and nanowires, whereas it represents the thickness in case of nanofilms.

$$\beta = \frac{6v_0}{0.0005736} \left(\frac{\sigma}{T_{mb}} \right) \quad (2)$$

Xie et al. [15] have developed another model by calculating surface-to-volume atomic ratio as a function of particle size. In this model, according to molar cohesive energy of nanoparticles and its linear relation with melting point, the following equation is suggested:

$$T_{mp} = T_{mb} \left(1 - \frac{3\alpha}{4} \right) \quad (3)$$

where α is surface-to-volume atomic ratio. Apparently, the key to calculate T_{mp} is to obtain α , which depends on the size and the shape of the nanosolid and atomic radius, r_0 . Eq. (4) expresses α

* Corresponding author. Tel./fax: +98 511 8763305.

E-mail addresses: jvahdati@iust.ac.ir, famirjalili@iust.ac.ir (J. Vahdati-Khaki).

values for different nanosolids:

$$\alpha = \frac{4r_0}{D}(3 - d) \quad (4)$$

where d is the dimension of crystal, $d = 0$ for nanoparticle, $d = 1$ for nanowire, and $d = 2$ for nanofilm. D is the particle diameter, wire diameter, or thickness of thin film.

In this work, a new concept of particle mean coordination number (MCN) will be introduced and a new model (MCN model) will be developed to calculate melting temperature of nanoparticles with free surfaces. With the use of MCN calculations more precise cohesive energy will be obtained for nanoparticles. According to the relation between melting temperature and cohesive energy, an expression for the size-dependent melting

temperature of nanoparticles will be developed. To confirm the efficiency of our new model, predictions for Al, Au, Pb, Ag, Cu, In, Sn, and Bi nanoparticles will be compared with the available experimental values and other theoretical models.

2. Model

One of the most critical characteristics of nanoparticles is their very high surface-to-volume ratio, i.e. large fractions of surface atoms. When the concentration of building blocks (atoms or ions) of a solid becomes sufficiently high, they aggregate into small clusters through homogeneous nucleation. With continuous supply of the building blocks, these clusters tend to coalesce and grow to form a larger cluster assembly. Clusters are structures with a central site around which the cluster is grown. The cluster may be considered as an onion-like structure (non-spherical) formed by several concentric shells around the central site. All the surface sites, which may belong to various shells, are defined as crusts. The number of crusts, n , defines the order of the cluster. The zeroth order corresponds to the central site. The first-order cluster is formed by adding a crust with a number of sites in such a way that they cover the central site and form a surface with a given geometrical shape such as cubo-octahedra (co), icosahedra (ico), body-centered cubic (bcc), and simple cubic (sc) (Fig. 1) [18]. The second-order cluster is formed by adding a crust over the first-order cluster, keeping the same geometrical shape as the first-order cluster. Clusters of higher order are formed in a similar way. Both co and ico clusters have close-packed structures; but in the ico the nearest neighbors on the same crust are at a shorter distance (5%) than those at adjacent crusts [18]. In addition to the mentioned geometrical shapes, there is a rarely formed cluster structure which is decahedra [1].

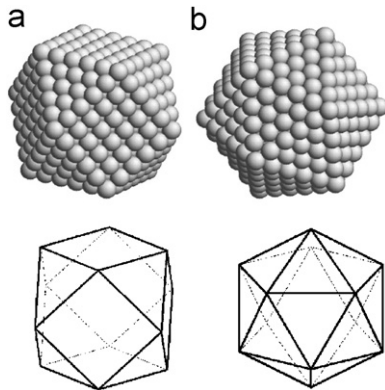


Fig. 1. Some geometrical structures of clusters: (a) cubo-octahedron and (b) icosahedron.

Table 1
Atomic parameters of a cluster with co, ico, bcc, and sc structure as a function of cluster order, n (based on [18])

Definition	Notation	Cluster structure			
		co	ico	bcc	sc
Total number of atoms	N	$10\frac{n^3}{3} + 5n^2 + 11\frac{n}{3} + 1$	$10\frac{n^3}{3} + 5n^2 + 11\frac{n}{3} + 1$	$(2n + 1)(n^2 + n + 1)$	$(2n + 1)^3$
Number of atoms in surface	N_s	$10n^2 + 2$	$10n^2 + 2$	$6n^2 + 2$	$24n^2 + 2$
Surface-to-volume atomic ratio	$\frac{N_s}{N}$	$\frac{30n^2 + 6}{10n^3 + 15n^2 + 11n + 3}$	$\frac{30n^2 + 6}{10n^3 + 15n^2 + 11n + 3}$	$\frac{6n^2 + 2}{(2n + 1)(n^2 + n + 1)}$	$\frac{24n^2 + 2}{(2n + 1)^3}$
Total number of cluster atomic bonds	N_b^c	$20n^3 + 15n^2 + 7n$	$20n^3 + 12n^2 + 4n$	$8n^3$	$24n^3 + 24n^2 + 6n$
Number of surface debonds	N_{db}^s	$30n^2 + 30n + 12$	$36n^2 + 36n + 12$	$24n^2 + 24n + 8$	$24n^2 + 24n + 6$
Total number of bulk atomic bonds	$N_b^b = N_b^c + \frac{1}{2}N_{db}^s$	$20n^3 + 30n^2 + 22n + 6$	$20n^3 + 30n^2 + 22n + 6$	$8n^3 + 12n^2 + 12n + 4$	$24n^3 + 36n^2 + 18n + 3$
Surface effective debonds-to-bulk bonds ratio	$\frac{(1/2)N_{db}^s}{N_b^b}$	$\frac{9n^2 + 9n + 3}{10n^3 + 15n^2 + 11n + 3}$	$\frac{15n^2 + 15n + 6}{20n^3 + 30n^2 + 22n + 6}$	$\frac{3n^2 + 3n + 1}{2n^3 + 3n^2 + 3n + 1}$	$\frac{4n^2 + 4n + 1}{8n^3 + 12n^2 + 6n + 1}$
Cluster-to-bulk atomic bond ratio	$\frac{N_b^c}{N_b^b}$	$\frac{10n^3 + 6n^2 + 2n}{10n^3 + 15n^2 + 11n + 3}$	$\frac{20n^3 + 15n^2 + 7n}{20n^3 + 30n^2 + 22n + 6}$	$\frac{2n^3}{2n^3 + 3n^2 + 3n + 1}$	$\frac{8n^3 + 8n^2 + 2n}{8n^3 + 12n^2 + 6n + 1}$
Bulk coordination number	$Z = \frac{2N_b^b}{N}$	12	12	8	6
Cluster mean coordination number	$\bar{Z} = \frac{2N_b^c}{N}$	$\frac{24n(5n^2 + 3n + 1)}{10n^3 + 15n^2 + 11n + 3}$	$\frac{6n(20n^2 + 15n + 7)}{10n^3 + 15n^2 + 11n + 3}$	$\frac{16n^3}{2n^3 + 3n^2 + 3n + 1}$	$\frac{12n}{2n + 1}$
Cluster-to-bulk mean coordination number ratio	$\frac{\bar{Z}}{Z}$	$\frac{2n(5n^2 + 3n + 1)}{10n^3 + 15n^2 + 11n + 3}$	$\frac{n(20n^2 + 15n + 7)}{20n^3 + 30n^2 + 22n + 6}$	$\frac{2n^3}{2n^3 + 3n^2 + 3n + 1}$	$\frac{2n}{2n + 1}$

For most transition metal nanoparticles these distinct structures can occur, which are not characteristics of the bulk crystal structure. Clusters with a small number of atoms (<150–200) crystallize in the form of ico. The structure becomes unstable for a large number of atoms and transforms to co, which is just a patch of the face-centered cubic (fcc) lattice [18].

The number of sites in a crust increases with the order, n , in a way that depends on the geometrical structure. There is a well-defined series for the number of sites as a function of the order, n , for each geometry. For co and ico clusters, the series are the same and it is given by 13, 55, 147, 309, 561, etc. On the other hand, the series for bcc and sc structures are 9, 35, 91, 189, etc. and 27, 125, 343, 729, etc. respectively [18]. It may be noted that we do not consider clusters with vacancies or defects. The relation between cluster order and its number of atoms is given in Table 1. Also other cluster parameters that are used to develop current new

model are shown in Table 1. Fig. 2 shows the variations of cluster MCN versus total number of atoms, N . Clearly MCN declines by reducing total number of atoms. Cluster-to-bulk coordination number ratio for different cluster structures is presented as a function of total number of atoms, N , in Fig. 3.

It is well known that both the cohesive energy and the melting temperature are parameters to describe the bond strength of materials. It is reported that the cohesive energy and melting temperature may have some proportional relations [12,19]. Assuming E_b and T_{mb} as molar cohesive energy and bulk melting point, following empirical relation of the melting temperature and molar cohesive energy is reported [19]:

$$T_{mb} = \frac{0.032}{k_B} E_b \quad (5)$$

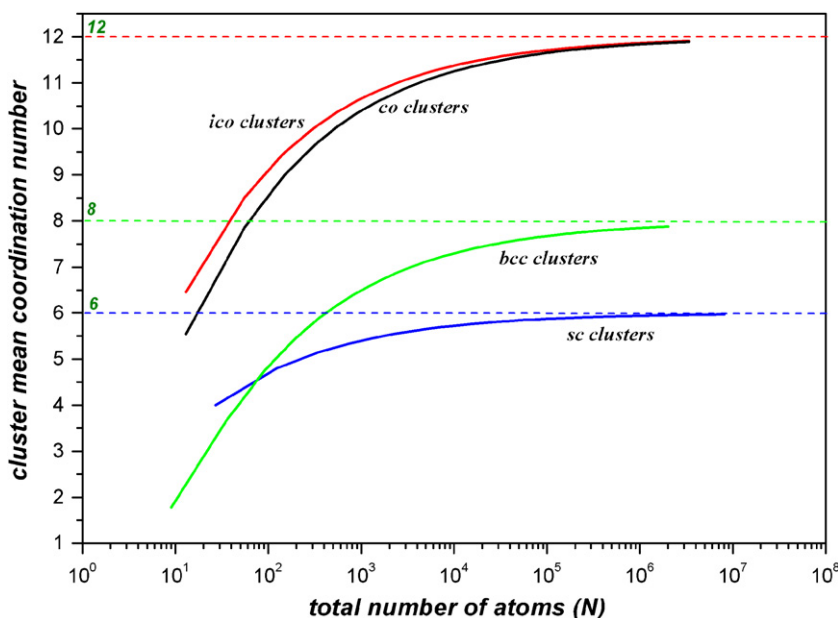


Fig. 2. Cluster mean coordination number as a function of total number of atoms, N .

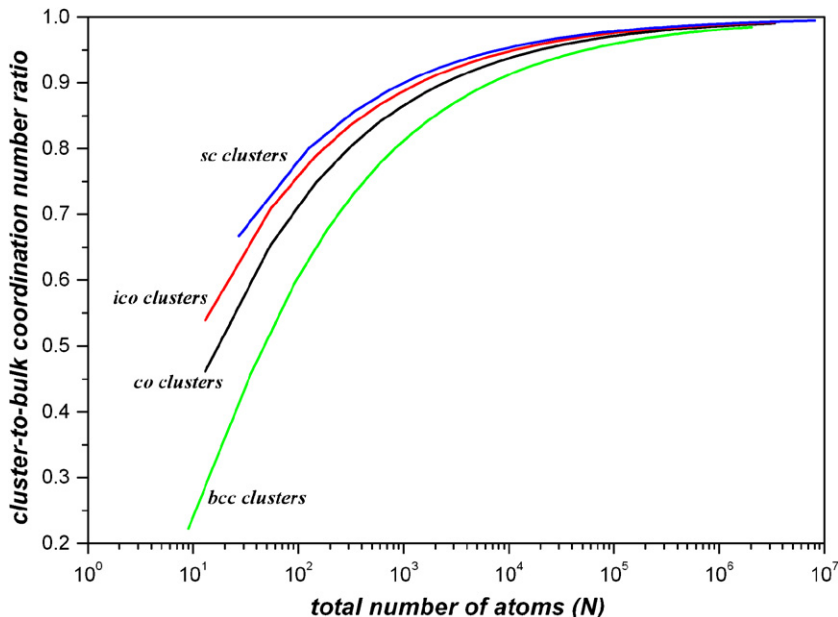


Fig. 3. Cluster-to-bulk coordination number ratio as a function of total number of atoms, N .

where k_B is Boltzmann's constant. In the same way, the melting point of a nanoparticle, T_{mp} , can be written as

$$T_{mp} = \frac{0.032}{k_B} E_p \quad (6)$$

where E_p is molar cohesive energy of nanoparticles atoms. The bulk molar cohesive energy, E_b , equals $N_a E_0$, where N_a is Avogadro's constant and E_0 is the cohesive energy per atom of the bulk material. Cohesive energy per atom is obtained by multiplying coordination number, Z , by half of bonding energy, $1/2 E_{bond}$, as each atomic bond is shared by two atoms:

$$E_b = N_a E_0 = \frac{1}{2} N_a Z E_{bond} \quad (7)$$

In the same way, molar cohesive energy of nanoparticles atoms can be written as

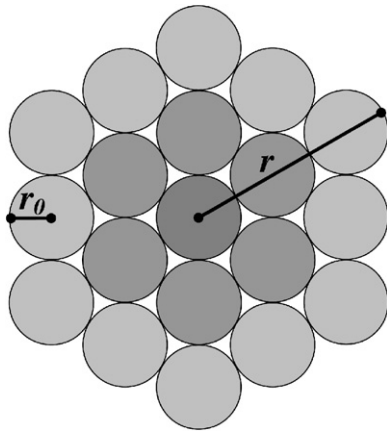


Fig. 4. The relation between particle size, r , and the cluster order, n , for a cubo-octahedral nanoparticle.

$$E_p = \frac{1}{2} N_a \bar{Z}_p E_{bond} \quad (8)$$

where \bar{Z}_p is the MCN of nanoparticles atoms. According to Eqs. (5)–(8), T_{mp} can be rewritten as

$$T_{mp} = T_{mb} \frac{\bar{Z}_p}{Z} \quad (9)$$

Considering Table 1, for different cluster structures the ratio of nanoparticles mean coordination number to bulk corresponding value can be defined as below. For a sc cluster, the equation is

$$\frac{\bar{Z}_p}{Z} = \frac{2n}{2n+1} \quad (10)$$

where n is the number of crusts (cluster order). On the other hand, for a bcc cluster, the ratio can be described by

$$\frac{\bar{Z}_p}{Z} = \frac{2n^3}{2n^3 + 3n^2 + 3n + 1} \quad (11)$$

In the same way, for an ico cluster we have

$$\frac{\bar{Z}_p}{Z} = \frac{n(20n^2 + 15n + 7)}{20n^3 + 30n^2 + 22n + 6} \quad (12)$$

As mentioned, ico structure is not stable for a large number of atoms and transforms to co. Therefore the most proper equation that could be used for close-packed materials is the one that corresponds to co clusters:

$$\frac{\bar{Z}_p}{Z} = \frac{2n(5n^2 + 3n + 1)}{10n^3 + 15n^2 + 11n + 3} \quad (13)$$

As shown in Fig. 4, the relation between particle size, r , and the number of crusts, n , could be deduced for a co nanoparticle by an inductive reasoning:

$$r = (2n + 1)r_0 \quad (14)$$

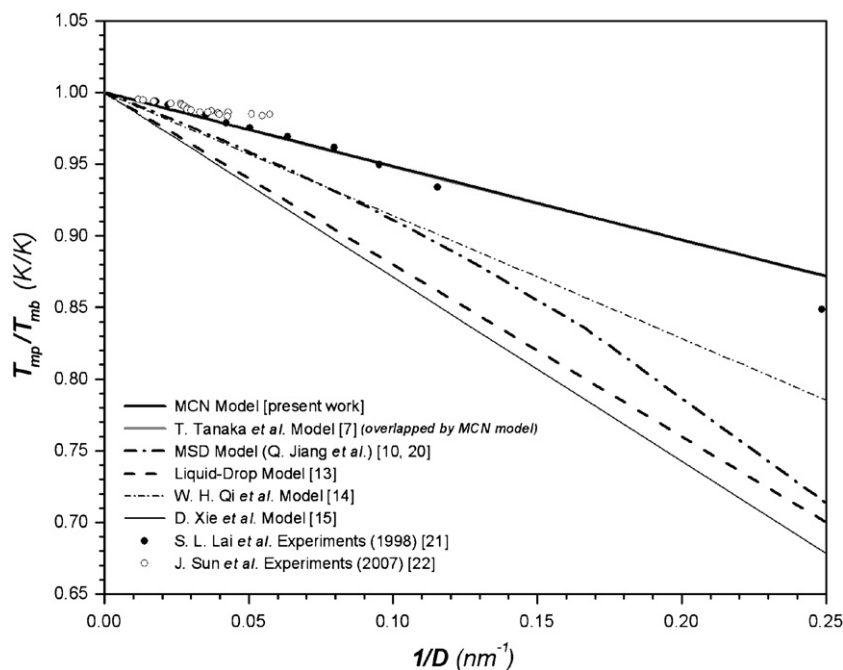


Fig. 5. Size-dependent melting point depression of Al nanoparticles versus reciprocal particle diameter, $1/D$. The melting temperature of bulk Al was taken as 933.25 K and the atomic radius as 0.143 nm. Bulk Al crystal structure is fcc [7,10,13–15,20–22].

where r_0 is atomic radius. Thus nanoparticle size-dependent melting point can be described as follows:

$$T_{mp} = T_{mb} \frac{2n(5n^2 + 3n + 1)}{10n^3 + 15n^2 + 11n + 3}, \quad n = \frac{1}{2}(r/r_0 - 1) \quad (15)$$

Ignoring the effect of curvature and surface relaxation, the above equation can be used for spherical close-packed nanoparticles with radius r . For non-close-packed nanoparticles same equations could be developed in the same manner.

3. Model verification and discussion

The main advantage of MCN model is that there is no need to know surface energies and other thermodynamic information. In our model only atomic radius and bulk melting temperature are needed for calculating nanoparticles melting point.

Size-dependant melting temperatures of Al, Au, Pb, Ag, Cu, In, Sn, and Bi nanoparticles are shown in Figs. 5–12 in comparison with some other models and experiments. The newly developed

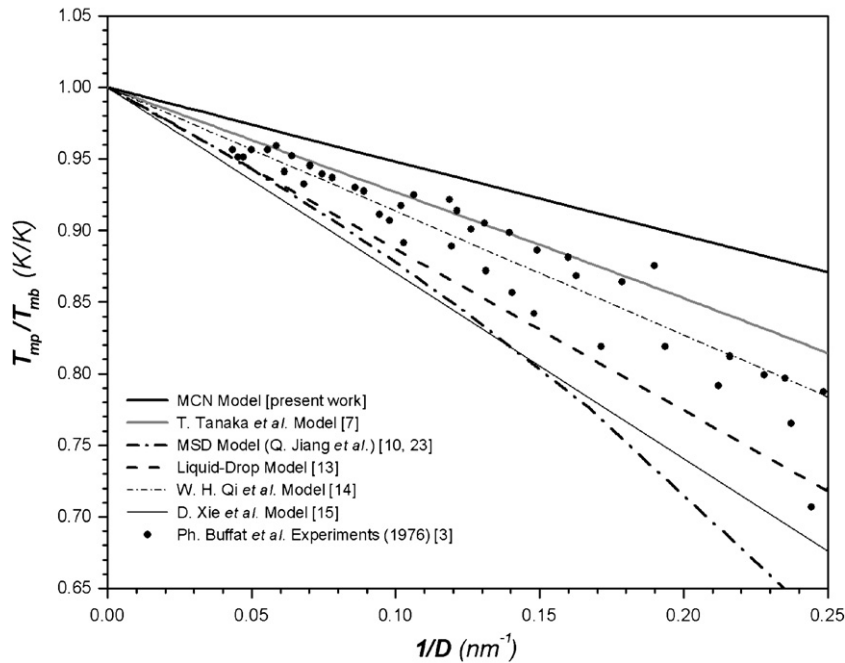


Fig. 6. Size-dependent melting point depression of Au nanoparticles versus reciprocal particle diameter, $1/D$. The melting temperature of bulk Au was taken as 1337.6 K and the atomic radius as 0.144 nm. Bulk Au crystal structure is fcc [3,7,10,13–15,23].

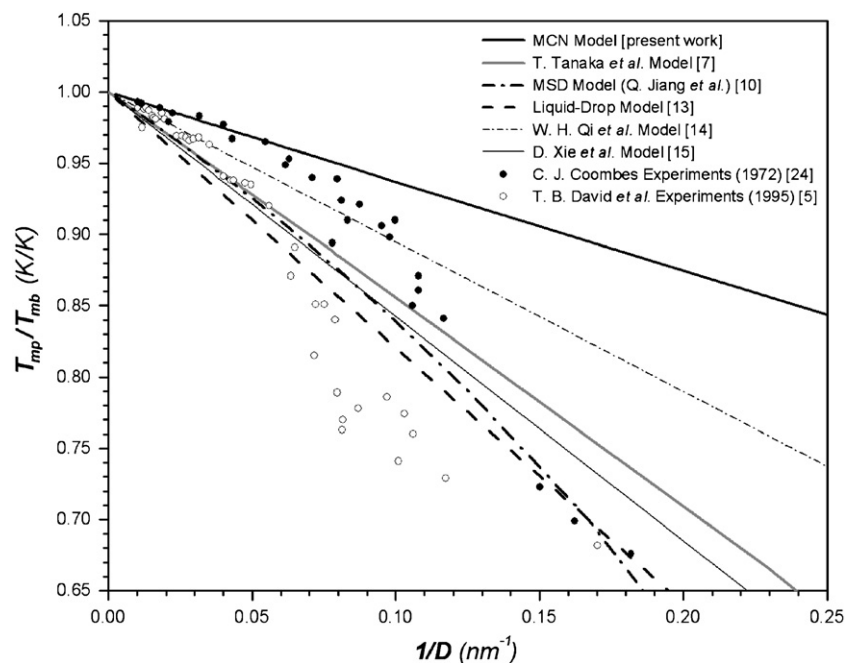


Fig. 7. Size-dependent melting point depression of Pb nanoparticles versus reciprocal particle diameter, $1/D$. The melting temperature of bulk Pb was taken as 600.6 K and the atomic radius as 0.175 nm. Bulk Pb crystal structure is fcc [5,7,10,13–15,24].

model is in good agreement with experimental values especially for Al and Pb. As it is clear for Pb and Sn, when size of particles decreases to diameters less than 20 nm, experimental values indicate a deviation from linear behavior. It may be caused by phenomena such as surface curvature, atomic relaxation, and surface contaminations. There are papers [30] that give us ideas to formulate surface relaxation effect on nanoparticles cohesive energy and melting temperature. Considering these effects we can improve our model to predict more accurately.

It seems metallic clusters are generally formed in co structures and they then transform into their bulk crystal structures as their sizes grow. Therefore Eq. (15) could be used for most of the metallic elements. Relevant equations for sc and bcc clusters can be derived from Eqs. (10) and (11). As illustrated for non-close-packed nanoparticles such as In and Sn, an acceptable prediction of size-dependant melting point is obtained by using Eq. (15); however, results for Bi are not so consistent with experimental values.

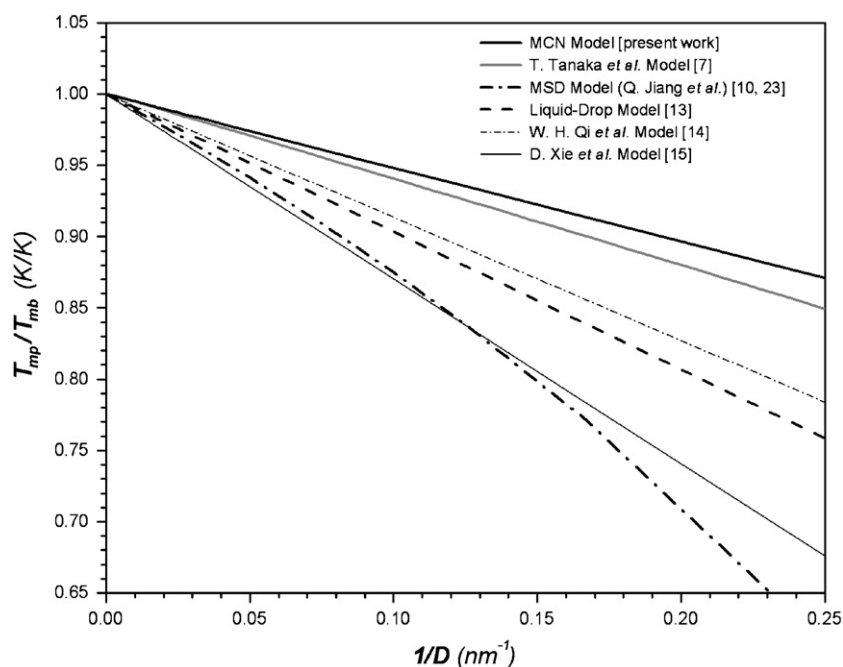


Fig. 8. Size-dependent melting point depression of Ag nanoparticles versus reciprocal particle diameter, $1/D$. The melting temperature of bulk Ag was taken as 1234 K and the atomic radius as 0.144 nm. Bulk Ag crystal structure is fcc [7,10,13–15,23].

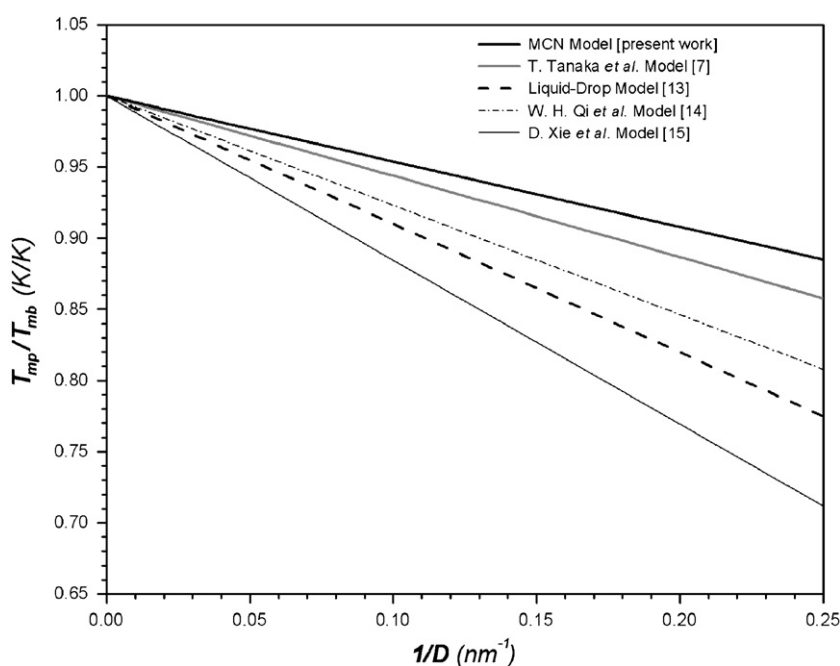


Fig. 9. Size-dependent melting point depression of Cu nanoparticles versus reciprocal particle diameter, $1/D$. The melting temperature of bulk Cu was taken as 1357.6 K and the atomic radius as 0.128 nm. Bulk Cu crystal structure is fcc [7,13–15].

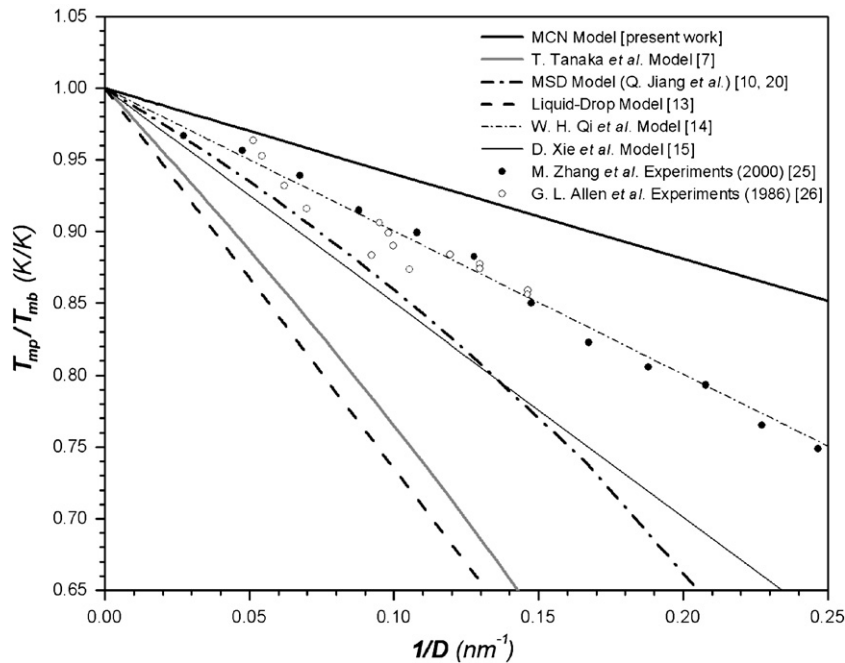


Fig. 10. Size-dependent melting point depression of In nanoparticles versus reciprocal particle diameter, $1/D$. The melting temperature of bulk In was taken as 933.25 K and the atomic radius as 0.166 nm. Bulk In crystal structure is tetragonal [7,10,13–15,20,25,26].

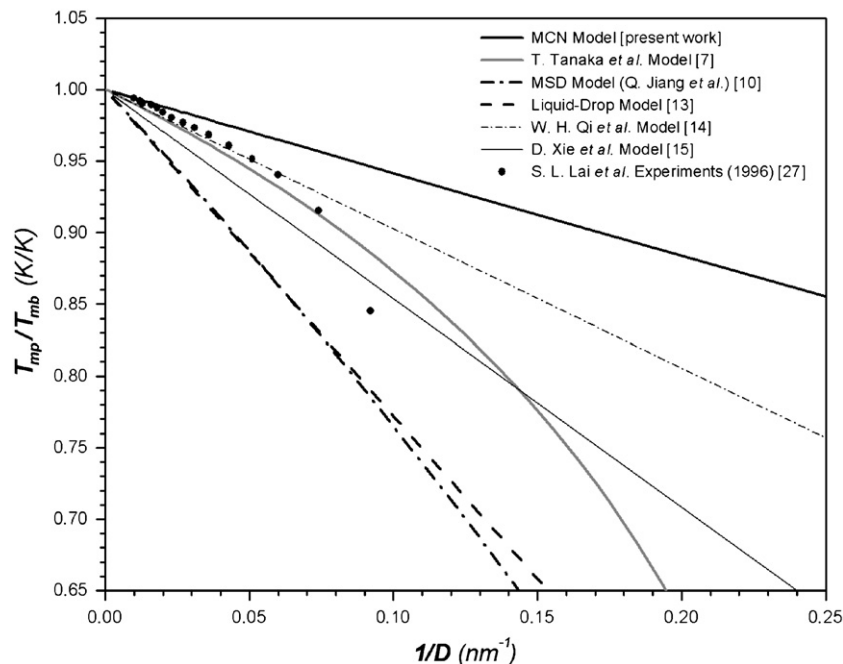


Fig. 11. Size-dependent melting point depression of Sn nanoparticles versus reciprocal particle diameter, $1/D$. The melting temperature of bulk Sn was taken as 505.06 K and the atomic radius as 0.162 nm. Bulk Sn crystal structure is tetragonal [7,10,13–15,27].

It is worth noting that according to MCN model (Eq. (15)) when atomic radius increases, the size dependency of melting point increases. Generally, according to this new model and other similar models, the following simple equation can be expressed for estimation of this dependency:

$$\frac{T_{mp}}{T_{mb}} = 1 - \frac{\kappa}{D} \quad (16)$$

where κ is a constant depending on material and can be calculated from MCN model by a linear data fitting method. The

κ magnitude reveals how much the melting point depends on particle size. The estimated values of κ for Al, Au, Pb, Ag, Cu, In, Sn, and Bi are 0.513, 0.517, 0.627, 0.517, 0.460, 0.595, 0.581, and 0.609 nm, respectively. This indicates that increasing atomic radius causes more size dependency of melting temperature. According to Eqs. (1) and (2), κ could be also used for the estimation of surface energy, σ . Considering Eq. (15), κ value for MCN model is approximately $1.8 D_0$, where D_0 is the atomic diameter. On the other hand, κ values for liquid-drop model (Eq. (1)) and Xie et al. model (Eq. (3)) equal β and $4.5 D_0$, respectively. Clearly MCN

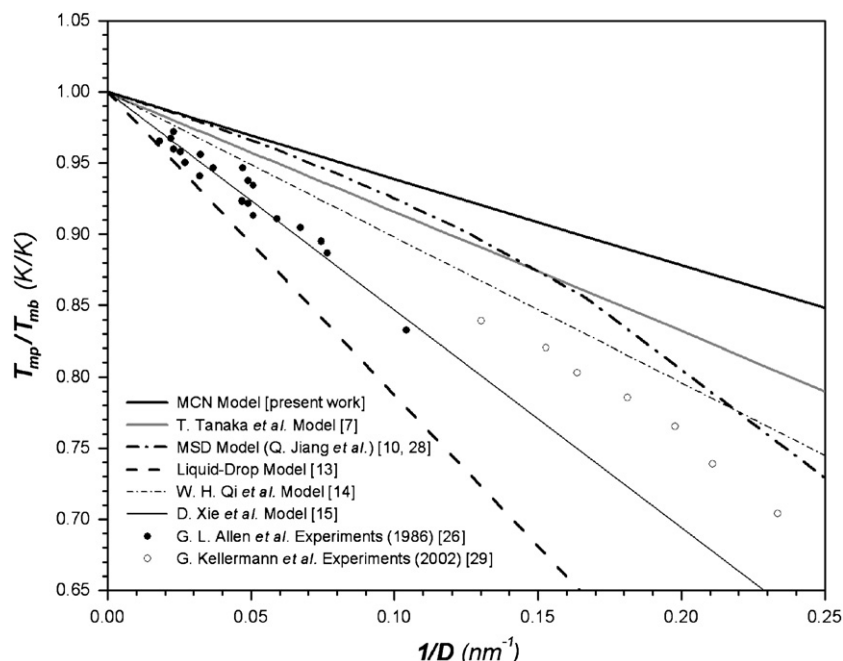


Fig. 12. Size-dependent melting point depression of Bi nanoparticles versus reciprocal particle diameter, $1/D$. The melting temperature of bulk Bi was taken as 544.52 K and the atomic radius as 0.170 nm. Bulk Bi crystal structure is rhombohedral [7,10,13–15,26,28,29].

model indicates less dependency on particle size as illustrated in Figs. 5–12.

4. Conclusions

In this work, a new model based on mean coordination number (MCN model) calculations was developed for predicting size-dependent melting point of nanoparticles. The model results for Al, Au, Pb, Ag, Cu, In, Sn, and Bi nanoparticles show the efficiency of this model in comparison with other models. According to MCN model it was found that for elements with the same crystal structure, size dependency of melting temperature increases with atomic radius. Considering the importance of the melting temperature of nanosolids, we are confident that the method presented in this paper may have potential application in the research on temperature-dependent properties of nanosolids.

Acknowledgments

We are grateful to T. Dallali-Isfahani, H. Amel-Farzad, and S. Raouf for useful discussions and helps.

References

- [1] S.C. Tjong, H. Chen, *Mater. Sci. Eng. R* 45 (2004) 1–88.
- [2] P. Pawlow, *Z. Phys. Chem.* 65 (1909) 1–35.
- [3] Ph. Buffat, J.P. Borel, *Phys. Rev. A* 13 (1976) 2287–2298.
- [4] T. Castro, R. Reifengerger, E. Choi, R.P. Andres, *Phys. Rev. B* 42 (1990) 8548–8557.
- [5] T.B. David, Y. Lereah, G. Deutscher, R. Kofman, P. Cheyssac, *Philos. Mag. A* 71 (1995) 1135–1143.
- [6] K.F. Peters, J.B. Cohen, Y.W. Chung, *Phys. Rev. B* 57 (1998) 13430–13438.
- [7] T. Tanaka, Sh. Hara, *Z. Metallkd.* 92 (2001) 467–472.
- [8] J. Sun, S.L. Simon, *Thermochim. Acta* 463 (2007) 32–40.
- [9] F.G. Shi, *J. Mater. Res.* 9 (1994) 1307–1313.
- [10] Q. Jiang, H.Y. Tong, D.T. Hsu, K. Okuyama, F.G. Shi, *Thin Solid Films* 312 (1998) 357–361.
- [11] Q. Jiang, Z. Zhang, J.C. Li, *Acta Mater.* 48 (2000) 4791–4795.
- [12] C.Q. Sun, Y. Wang, B.K. Tay, S. Li, H. Huang, Y.B. Zhang, *J. Phys. Chem. B* 106 (2002) 10701–10705.
- [13] K.K. Nanda, S.N. Sahu, S.N. Behera, *Phys. Rev. A* 66 (2002) 013208.
- [14] W.H. Qi, M.P. Wang, *Mater. Chem. Phys.* 88 (2004) 280–284.
- [15] D. Xie, M.P. Wang, W.H. Qi, L.F. Cao, *Mater. Chem. Phys.* 96 (2006) 418–421.
- [16] W.H. Qi, M.P. Wang, M. Zhou, X.Q. Shen, X.F. Zhang, *J. Phys. Chem. Solids* 67 (2006) 851–855.
- [17] W.H. Qi, M.P. Wang, *Mater. Lett.* 59 (2005) 2262–2266.
- [18] J.M. Montejano-Carrizales, F. Aguilera-Granja, J.L. Moran-Lopez, *Nanostruct. Mater.* 8 (1997) 269–287.
- [19] F. Guinea, J.H. Rose, J.R. Smith, J. Ferrante, *Appl. Phys. Lett.* 44 (1984) 53–55.
- [20] Q. Jiang, Z. Zhang, Y.W. Wang, *Mater. Sci. Eng. A* 286 (2000) 139–143.
- [21] S.L. Lai, J.R.A. Carisson, L.H. Allen, *Appl. Phys. Lett.* 72 (1998) 1098–1100.
- [22] J. Sun, S.L. Simon, *Thermochim. Acta* 463 (2007) 32–40.
- [23] Q. Jiang, S. Zhang, M. Zhao, *Mater. Chem. Phys.* 82 (2003) 225–227.
- [24] C.J. Coombes, *J. Phys. F: Metal. Phys.* 2 (1972) 441–449.
- [25] M. Zhang, M.Y. Efremov, F. Schiettekatte, E.A. Olson, A.T. Kwan, S.L. Lai, T. Wisleder, J.E. Greene, L.H. Allen, *Phys. Rev. B* 62 (2000) 10548–10557.
- [26] G.L. Allen, R.A. Bayles, W.W. Gile, W.A. Jesser, *Thin Solid Films* 144 (1986) 297–308.
- [27] S.L. Lai, J.Y. Guo, V. Petrova, G. Ramanath, L.H. Allen, *Phys. Rev. Lett.* 77 (1996) 99–102.
- [28] L.H. Liang, J.C. Li, Q. Jiang, *Physica B* 334 (2003) 49–53.
- [29] G. Kellermann, A.F. Craievich, *Phys. Rev. B* 65 (2002) 134204–134209.
- [30] D. Xie, M.P. Wang, W.H. Qi, *J. Phys.: Condens. Matter* 16 (2004) L401–L405.